

New Eco-Friendly Corrosion Inhibitors Based on Phenolic Derivatives for Protection Mild Steel Corrosion

A.S.Fouda^{1,*}, A.M.Eldesoky², M.A.Elmosri³, T.A.Fayed³ and M.F.Atia³

¹Department of Chemistry, Faculty of Science, El-Mansoura University, El-Mansoura-35516, Egypt:

²Engineering Chemistry Department, High Institute of Engineering & Technolog (New Damietta),

³Department of Chemistry, Faculty of Science, Tanta University, Egypt

*E-mail: asfouda@hotmail.com

Received: 30 May 2013 / Accepted: 2 July 2013 / Published: 1 August 2013

Some phenolic derivatives such as: 4-(5-(4-dimethylamino) phenyl)-1 H-pyrazol-5-yl)phenol and 4-(5-(4-nitrophenyl)-1 H-pyrazol-5-yl)phenol were investigated as corrosion inhibitors for mild steel in 1 M HCl solution. Electrochemical impedance spectroscopy (EIS), potentiodynamic polarization, scanning electron microscope technology with energy dispersive X-ray spectroscopy (SEM–EDX) and weight loss methods were used to study the inhibition action at 30°C. The corrosion of mild steel was controlled by a charge transfer process at the prevailing conditions. The electrochemical results showed that these compounds are efficient inhibitors for mild steel and efficiency up to 85.0 % was obtained at 30°C. The inhibition efficiency increases with inhibitor concentration. The adsorption of these compounds on mild steel surface follows the Frumkin adsorption isotherm. The increase of inhibitor efficiency with increasing the concentration can be interpreted on the basis of the adsorption amount and the coverage of phenolic molecules, increases with increasing concentration. Polarization curves indicate that investigated phenolic derivatives are mixed-type inhibitors. The Kinetic parameters of corrosion processes were calculated and discussed. The chemical and electrochemical methods gave similar results.

Keywords: Corrosion inhibition, mild steel, phenolic derivatives, HCl, SEM, EDX

1. INTRODUCTION

Mild steel has been extensively used under different conditions in petroleum industries [1]. Aqueous solutions of acids are among the most corrosive media and are widely used in industries for pickling, acid cleaning of boilers, descaling and oil well [2, 6]. The main problem concerning mild steel applications is its relatively low corrosion resistance in acidic solution. Several methods used currently to reduce corrosion of mild steel. One of such methods is the use of organic inhibitors [7-

17]. Effective inhibitors are heterocyclic compounds that have π bonds, heteroatoms such as sulphur, oxygen and nitrogen [18]. Compounds containing both nitrogen and chloro atoms can provide excellent inhibition, compared with compounds containing only nitrogen or chloro atom [19]. Heterocyclic compounds such as phenolic can provide excellent inhibition. These molecules depends mainly on certain physical properties of the inhibitor molecules such as functional groups, steric factors, electron density at the donor atom and electronic structure of the molecules [20, 21]. Regarding the adsorption of the inhibitor on the metal surface, two types of interactions are responsible. One is physical adsorption which involves electrostatic force between ionic charges or dipoles of the adsorbed species and electric charge at metal/ solution interface. Other is chemical adsorption, which involves charge sharing or charge transfer from inhibitor molecules to the metal surface to form coordinated types of bonds [22]. The selection of appropriate inhibitors mainly depends on the type of acid, its concentration, and temperature.

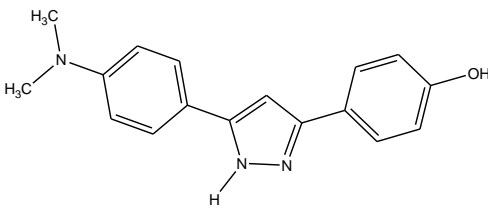
In the present work, the inhibition characteristics of 4-(5-(4-dimethylamino)phenyl)-1 H-pyrazol-5-yl)phenol and 4-(5-(4-nitrophenyl)-1 H-pyrazol-5-yl)phenol were investigated as corrosion inhibitors for mild steel in 1 M HCl solution using chemical and electrochemical techniques.

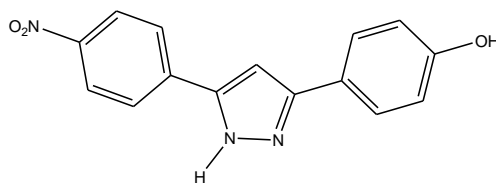
2. EXPERIMENTAL

2.1. Chemicals and materials

Hydrochloric acid (37 %) ,ethyl alcohol and acetone were purchased from Al-gomhoria Company, Egypt, 4-(5-(4-dimethylamino)phenyl)-1 H-pyrazol-5-yl)phenol and 4-(5-(4-nitrophenyl)-1 H-pyrazol-5-yl) phenol were synthesized as described before [23] and the purity of the compounds was checked by TLC. The molecular structures and other details of these compounds are given in Table (1). Bidistilled water was used throughout all the experiments.

Table 1. Molecular structures, formulas and molecular weights of investigated compounds

| Inhibitors | Structures | Mol. Formulas & Mol. Weights |
|--|--|------------------------------|
| Compound (A) 4-(5-(4-dimethylamino)phenyl)-1H-pyrazol-5-yl)phenol |  | $C_{17}H_{17}N_3O$ 279.34 |

Compound (B)**4-(5-(4-nitrophenyl)-1 H-pyrazol-5-yl) phenol**
 $C_{15}H_{11}N_3O_3$
 281.27

The composition of mild steel (weight %) is given in Table (2):

Table 2. Chemical composition of mild steel (weight %):

| Chemical constituent | C | Cr | Ni | Si | Mn | P | S | Fe |
|----------------------|-------------|-----|------|------|-----|------|------|------|
| Composition (wt %) | 0.14 – 0.20 | 0.1 | 0.01 | 0.24 | 0.5 | 0.05 | 0.05 | rest |

2.2. Methods

2.2.1. Weight loss measurements

Rectangular specimens of mild steel with dimensions 2.1 x 2.0 x 0.2 cm were abraded with different grades of emery paper, degreased with acetone, rinsed with bidistilled water and dried between filter papers. After weighting accurately, the specimens were immersed in 100 ml of 1 M HCl with and without different concentrations of inhibitors at 30 °C. After different immersion periods (each of 30 min till 180 min), the mild steel samples were taken out, washed with bidistilled water, dried and weighted again. The weight loss values are used to calculate the corrosion rate (R) in mm^{-1} by Eq. (1):

$$R = (\text{weight loss in gram} \times 8.75 \times 10^4) / DAT \quad (1)$$

where D is carbon steel density in g cm^{-3} , A is exposed area in cm^2 , T is exposure time in hr.

The inhibition efficiency (% Y_w) and the degree of surface coverage (θ) were calculated from Eq. (2):

$$\% Y_w = \theta \times 100 = [(R^* - R) / R^*] \times 100 \quad (2)$$

where R^* and R are the corrosion rates of mild steel in the absence and in the presence of inhibitor, respectively.

2.2.2. Electrochemical measurements

Electrochemical measurements were conducted in a conventional three electrodes thermostated cell assembly using an Gamry potentiostat/galvanostat/ZRA (model PCI300/4). A platinum foil and saturated calomel electrode (SCE) were used as counter and reference electrodes, respectively. The

mild steel electrodes were 1x1 cm and were welded from one side to a copper wire used for electrical connection. The electrodes were abraded, degreased and rinsed as described in weight loss measurements. All experiments were carried out at temperature $(30 \pm 1^\circ\text{C})$. The potentiodynamic curves were recorded from -500 to 500 mV at a scan rate 1 mV S^{-1} after the steady state is reached (30 min) and the open circuit potential (OCP) was noted. The % Y_p and degree of surface coverage were calculated from Eq. (3):

$$Y_p\% = \theta \times 100 = [1 - (i_{\text{corr}}^0 / i_{\text{corr}})] \times 100 \quad (3)$$

where i_{corr}^0 and i_{corr} are the corrosion current densities of uninhibited and inhibited solution, respectively.

Electrochemical impedance spectroscopy (EIS) and electrochemical frequency modulation (EFM) experiments were carried out using the same instrument as before with a Gamry framework system based on ESA400. Gamry applications include software EIS300 for EIS measurements and EFM140 for EFM measurements; computer was used for collecting data. Echem Analyst 5.5 Software was used for plotting, graphing and fitting data. EIS measurements were carried out in a frequency range of 100 kHz to 10 mHz with amplitude of 5 mV peak-to-peak using ac signals at respective corrosion potential. EFM carried out using two frequencies 2 and 5 Hz. The base frequency was 1 Hz. In this study, we use a perturbation signal with amplitude of 10 mV for both perturbation frequencies of 2 and 5 Hz.

2.2.3. SEM-EDX Measurement

The mild steel surface was prepared by keeping the specimens for 3 days immersion in 1 M HCl in the presence and absence of optimum concentrations of investigated derivatives, after abraded using different emery papers up to 1200 grit size. Then, after this immersion time, the specimens were washed gently with bidistilled water, carefully dried and mounted into the spectrometer without any further treatment. The corroded mild steel surfaces were examined using an X-ray diffractometer Philips (pw-1390) with Cu-tube (Cu Ka1, $\lambda = 1.54051 \text{ \AA}$), a scanning electron microscope (SEM, JOEL, JSM-T20, Japan).

2.2.4. Theoretical study

Accelrys (Material Studio Version 4.4) software for quantum chemical calculations has been used.

3. RESULTS AND DISCUSSION

3.1. Weight loss measurements

Figure (1) shows the weight loss–time curves for the corrosion of mild steel in 1 M HCl in the absence and presence of different concentrations of compound (A). Similar curves for compound (B)

were obtained and are not shown. The data of Table (3) show that, the inhibition efficiency increases with increase in inhibitor concentration from 1×10^{-6} to 21×10^{-6} M. The maximum inhibition efficiency was achieved at 21×10^{-6} M. The lowest inhibition efficiency (% Y_w) is obtained in the presence of compound (B), therefore % Y_w tends to decrease in the following order: compound (A) > compound (B).

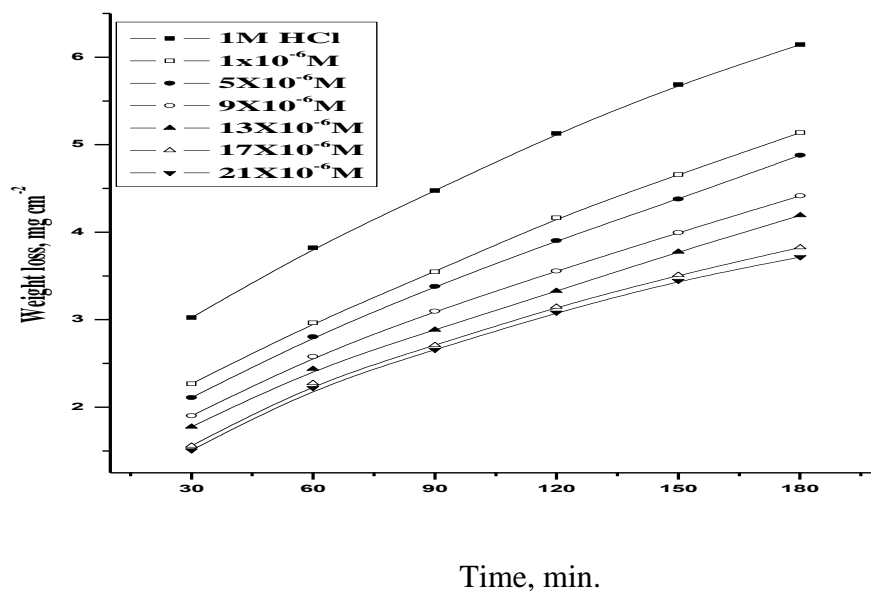


Figure 1. Weight loss-time curves for mild steel dissolution in 1M HCl in absence and presence of different concentrations of compound (A) at 30 °C

Table 3. Data of weight loss measurements for mild in 1 M HCl solution in the absence and presence of different concentrations of investigated compounds at 30 °C

| Compound | Conc., M | θ | % Y_w |
|--------------|---------------------|----------|---------|
| Blank | 0.00 | ----- | ----- |
| A | 1×10^{-6} | 0.504 | 50.4 |
| | 5×10^{-6} | 0.544 | 54.4 |
| | 9×10^{-6} | 0.581 | 58.1 |
| | 13×10^{-6} | 0.624 | 62.4 |
| | 17×10^{-6} | 0.653 | 65.3 |
| | 21×10^{-6} | 0.699 | 69.9 |
| B | 1×10^{-6} | 0.360 | 36.0 |
| | 5×10^{-6} | 0.382 | 38.2 |
| | 9×10^{-6} | 0.431 | 43.1 |
| | 13×10^{-6} | 0.481 | 48.1 |
| | 17×10^{-6} | 0.530 | 53.0 |
| | 21×10^{-6} | 0.550 | 55.0 |

3.2. Electrochemical measurements

3.2.1. Potentiodynamic polarization measurements

The potentiodynamic curves for mild steel in 1 M HCl in the absence and presence of compound (A) are shown in Fig. (2). Similar curves were obtained for compound (B) (not shown). It is clear that; the investigated inhibitors affect the promoting retardation of anodic dissolution of mild steel and cathodic hydrogen discharge reactions. Electrochemical parameters such as corrosion current density (i_{corr}), corrosion potential (E_{corr}), Tafel constants (β_a and β_c), degree of surface coverage (θ) and inhibition efficiency ($\% Y_p$) were calculated from Tafel plots and are given in Table (4). It is observed that the presence of inhibitor lowers i_{corr} . Maximum decrease in i_{corr} values was observed for compound (A) indicating that this is the most effective corrosion inhibitor. It is also observed from Table (4) that E_{corr} values and Tafel slopes do not change significantly in inhibited solution as compared to uninhibited solution. The investigated compounds do not shift the E_{corr} values significantly, suggesting that they behave as mixed type inhibitors [24]. Both cathodic (β_c) and anodic Tafel lines (β_a) are parallel and are shifted to more negative and positive direction, respectively by adding inhibitors. This is indicating that the mechanism of the corrosion reaction does not change and the corrosion reaction is inhibited by simple adsorption mode [25]. The irregular trends of β_a and β_c values indicate the involvement of more than one type of species adsorbed on the metal surface. The order of inhibition efficiency was found to be (Table 4): compound (A) > compound (B).

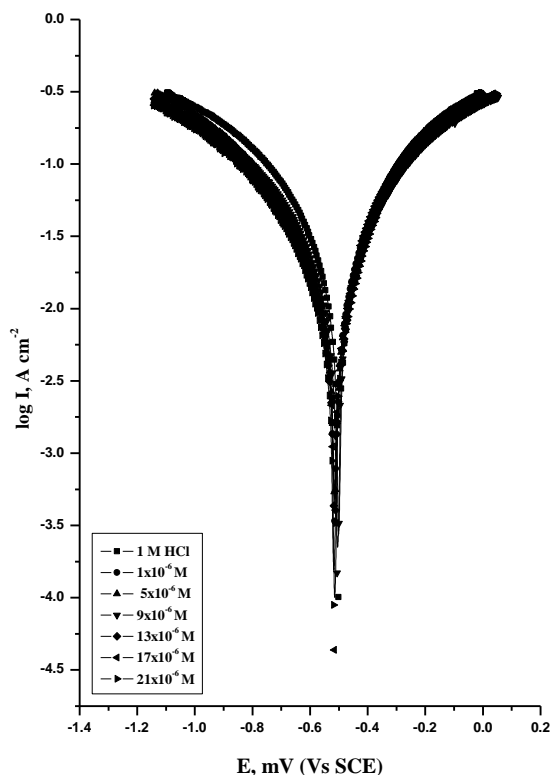


Figure 2. Potentiodynamic polarization curves for the corrosion of mild steel in 1 M HCl in the absence and presence of various concentrations of compound (A) at 30°C

Table 4. Potentiodynamic data of mild steel in 1M HCl and in the presence of different concentrations of inhibitors at 30°C

| Comp. | Conc., M | $-E_{\text{corr}}$, mVvs. SCE, | i_{corr} $\mu\text{A cm}^{-2}$ | $-\beta_c$, mVdec^{-1} | β_a , mVdec^{-1} | Θ | $Y_P\%$ |
|---------------------|---------------------|---------------------------------------|--|-------------------------------------|------------------------------------|----------|---------|
| Blank | 0.0 | 501 | 45.9 | 675 | 557 | --- | ---- |
| A | 1×10^{-6} | 503 | 15.0 | 493 | 410 | 0.673 | 67.3 |
| | 5×10^{-6} | 506 | 12.6 | 467 | 384 | 0.725 | 72.5 |
| | 9×10^{-6} | 508 | 10.6 | 449 | 360 | 0.769 | 76.9 |
| | 13×10^{-6} | 510 | 9.0 | 442 | 361 | 0.803 | 80.3 |
| | 17×10^{-6} | 511 | 8.1 | 429 | 340 | 0.823 | 82.3 |
| | 21×10^{-6} | 515 | 6.6 | 391 | 312 | 0.856 | 85.6 |
| | B | 1×10^{-6} | 512 | 37.8 | 680 | 589 | 0.176 |
| 5×10^{-6} | | 518 | 34.1 | 654 | 533 | 0.257 | 25.7 |
| 9×10^{-6} | | 514 | 32.3 | 658 | 517 | 0.296 | 29.6 |
| 13×10^{-6} | | 514 | 28.7 | 629 | 494 | 0.374 | 37.4 |
| 17×10^{-6} | | 516 | 26.0 | 604 | 475 | 0.433 | 43.3 |
| 21×10^{-6} | | 512 | 25.3 | 567 | 454 | 0.448 | 44.8 |

3.2.2. Electrochemical impedance spectroscopy

The EIS provides important mechanistic and kinetic information for an electrochemical system under investigation. Nyquist impedance plots obtained for the mild steel electrode at respective corrosion potentials after 30 min immersion in 1M HCl in presence and absence of various concentrations of compound (A) is shown in Fig.3 (compound (B) curves not shown). This diagram exhibits a single semi-circle shifted along the real impedance (Z_r). The Nyquist plots of compound (A) do not yield perfect semicircles as expected from the theory of EIS, the impedance loops measured are depressed semi-circles with their centers below the real axis, where the kind of phenomenon is known as the “dispersing effect” as a result of frequency dispersion [26] and mass transport resistant [27] as well as electrode surface heterogeneity resulting from surface roughness, impurities, dislocations, grain boundaries, adsorption of inhibitors, formation of porous layers [28–32], etc. so one constant phase element (CPE) is substituted for the capacitive element, to explain the depression of the capacitance semi-circle, to give a more accurate fit. Impedance data are analyzed using the circuit in Fig.(4); in which R_s represents the electrolyte resistance, R_{ct} represents the charge-transfer resistance and the

constant phase element (CPE). According to Hsu and Mansfeld [33] the correction of capacity to its real values is calculated from Eq. (6):

$$C_{dl} = Y_o (\omega_{max})^{n-1} \tag{6}$$

where Y_o is the CPE coefficient, ω_{max} is the frequency at which the imaginary part of impedance ($-Z_i$) has a maximum and n is the CPE exponent (phase shift).

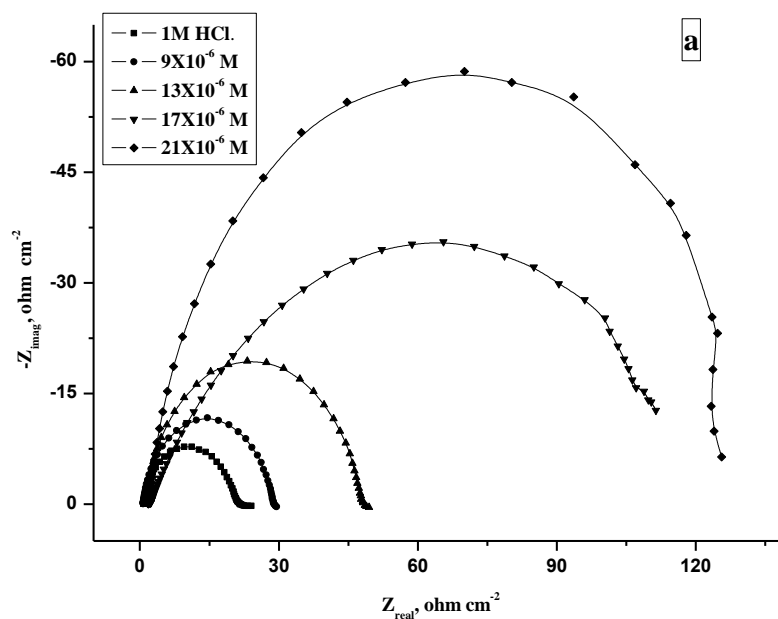
The data obtained from fitted spectra are listed in Table (5). The $Y_I\%$ was calculated from Eq. (7):

$$Y_I\% = \frac{R_{ct} - R_{ct}^*}{R_{ct}} \times 100 \tag{7}$$

where R_{ct} and R_{ct}^* are the charge-transfer resistances with and without the inhibitors, respectively.

Data in Table (5) show that; the R_s values are very small compared to the R_{ct} values. Also; the R_{ct} values increase and the calculated C_{dl} values decrease by increasing the inhibitor concentrations, which causes an increase of θ and Y_I . The high R_{ct} values are generally associated with slower corroding system [34]. The decrease in the C_{dl} suggests that inhibitors function by adsorption at the metal/solution interface [35].

The inhibition efficiencies, calculated from EIS results, show the same trend as those obtained from polarization measurements. The difference of inhibition efficiency from two methods may be attributed to the different surface status of the electrode in two measurements. EIS were performed at the rest potential, while in polarization measurements the electrode potential was polarized to high over potential, non-uniform current distributions, resulted from cell geometry, solution conductivity, counter and reference electrode placement, etc., will lead to the difference between the electrode area actually undergoing polarization and the total area [36].



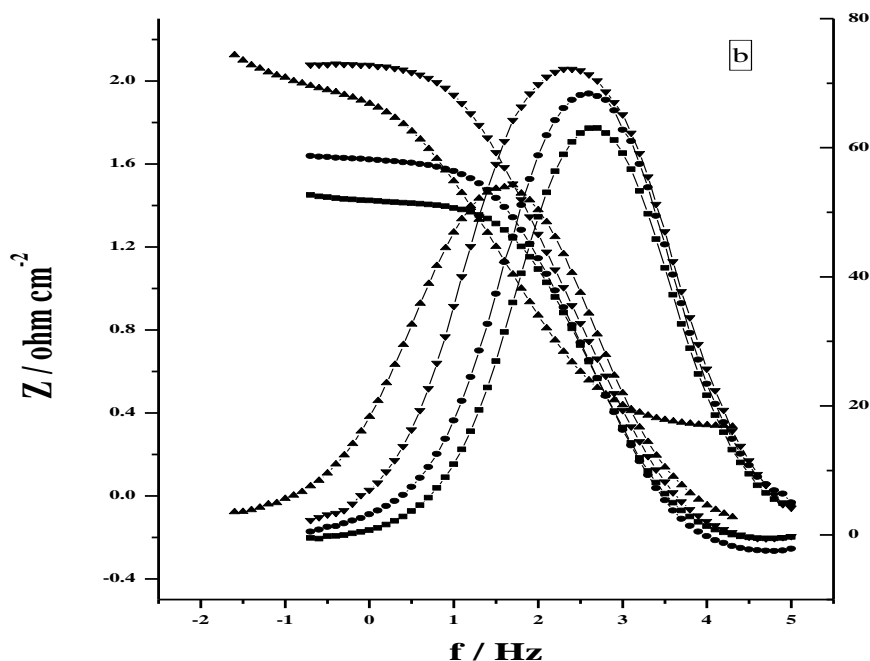


Figure 3. The Nyquist (a) and Bode (b) plots for corrosion of mild steel in 1M HCl in the absence and presence of different concentrations of compound (A) at 30°C

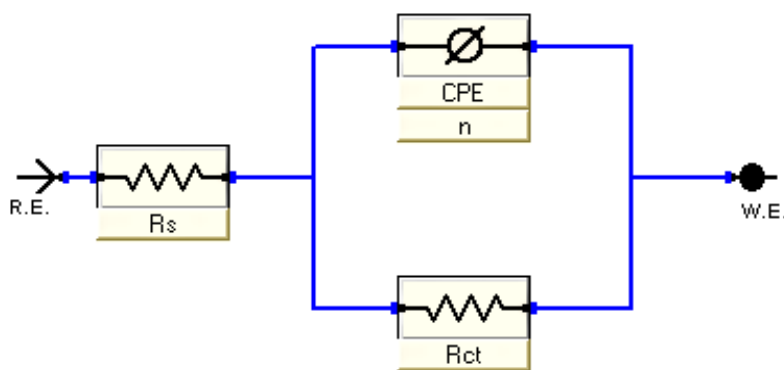


Figure 4. Equivalent circuit model used to fit the impedance spectra data

Table 5. EIS data of mild steel in the presence and absence of different concentrations of inhibitors at 30°C

| Compound | Conc., M | R_{CT} $\Omega \text{ cm}^2$ | C_{dl} $\mu\text{F cm}^{-2}$ | θ | $\%Y_1$ |
|----------|----------|-----------------------------------|-----------------------------------|----------|---------|
| Blank | 0.0 | 95.22 | 21.7 | ---- | ---- |

| | | | | | |
|---|---------------------|-------|-------|-------|------|
| A | 9×10^{-6} | 92.51 | 31.0 | 0.30 | 30.0 |
| | 13×10^{-6} | 92.20 | 49.5 | 0.561 | 56.1 |
| | 17×10^{-6} | 86.55 | 117.3 | 0.815 | 81.5 |
| | 21×10^{-6} | 82.56 | 133.0 | 0.836 | 83.6 |
| B | 9×10^{-6} | 87.70 | 24.0 | 0.095 | 9.50 |
| | 13×10^{-6} | 86.01 | 38.3 | 0.433 | 43.3 |
| | 17×10^{-6} | 82.23 | 80.7 | 0.731 | 73.1 |
| | 21×10^{-6} | 77.05 | 106.1 | 0.795 | 79.5 |

3.2.3. Adsorption isotherm

One of the most convenient ways of expressing adsorption quantitatively is by deriving the adsorption isotherm that characterizes the metal/inhibitor/ environment system [37]. The surface coverage (θ) values were tested graphically to allow fitting of a suitable adsorption isotherm. The plot of θ versus $\log C$ [Fig. (5)] yielded S-shape curve clearly proving that the adsorption of these inhibitors from 1 M HCl solution on mild steel surface obeys Frumkin adsorption isotherm:

$$K_{ads}C = (\theta/1-\theta) \exp (-2 a \theta) \tag{9}$$

Where K_{ads} is the adsorption equilibrium constant, a is the interaction parameter and C is the inhibitor concentration.

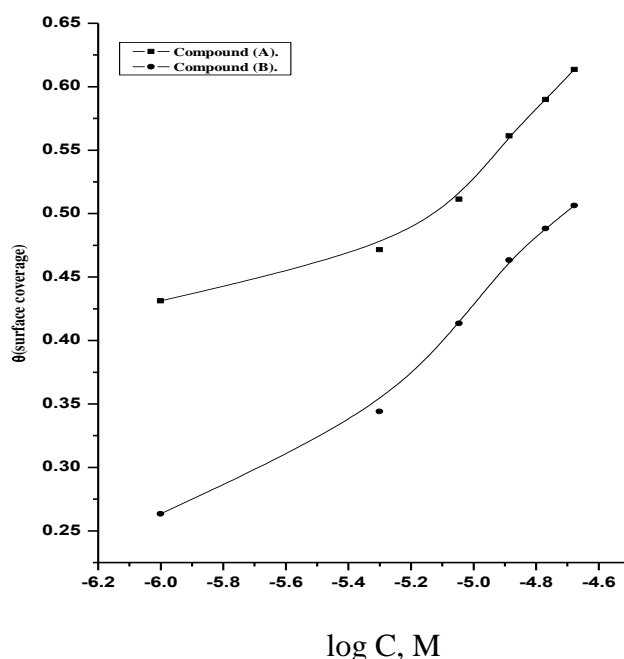


Figure (5): θ - $\log C$ curves for mild steel dissolution in 1M HCl in presence of different compounds from weight loss measurements at 30°C

3.1.4- Kinetic parameters

The effect of temperature (30 – 60°C) on the performance of the inhibitors at different concentrations of (1×10^{-6} - 21×10^{-6} M) for mild steel in 1M HCl was studied using weight-loss measurements. Plot of log k (corrosion rate) against 1/ T (absolute temperature) Fig. (6) for mild steel in 1M M HCl, gave straight lines. The values of the slopes obtained at different temperatures permit the calculation of Arrhenius activation energy (E_a^*). Kinetic parameters for corrosion of mild steel were calculated from Arrhenius – type plot.

$$k = A \exp (-E_a^* / RT) \tag{9}$$

and transition state- type equation :

$$k = RT / Nh \exp (\Delta S^*/R) \exp (-\Delta H^* / RT) \tag{10}$$

The relation between log k / T vs. 1 / T gives straight line, from its slope, ΔH^* can be computed and from its intercept ΔS^* can be also computed Fig (7).

Table (6) exhibits the values of apparent activation energy E_a^* , enthalpies ΔH^* and entropies ΔS^* for mild steel dissolution in 1M HCl solution. The presence of phenolic derivatives increases the activation energies of mild steel indicating strong adsorption of the phenolic molecules on the metal surface and the presence of these additives induces energy barrier for the corrosion reaction and this barrier increases with increasing the additive concentrations.

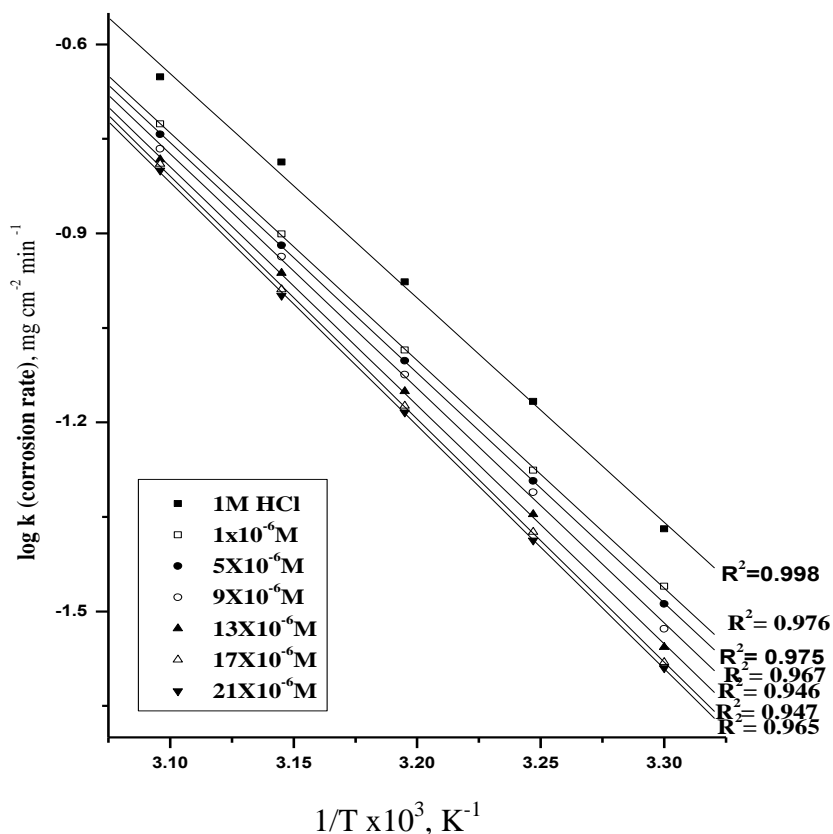


Figure 6. log k (corrosion rate) - 1/T curves for mild steel dissolution in 1M HCl in absence and presence of different concentrations of compound (A)

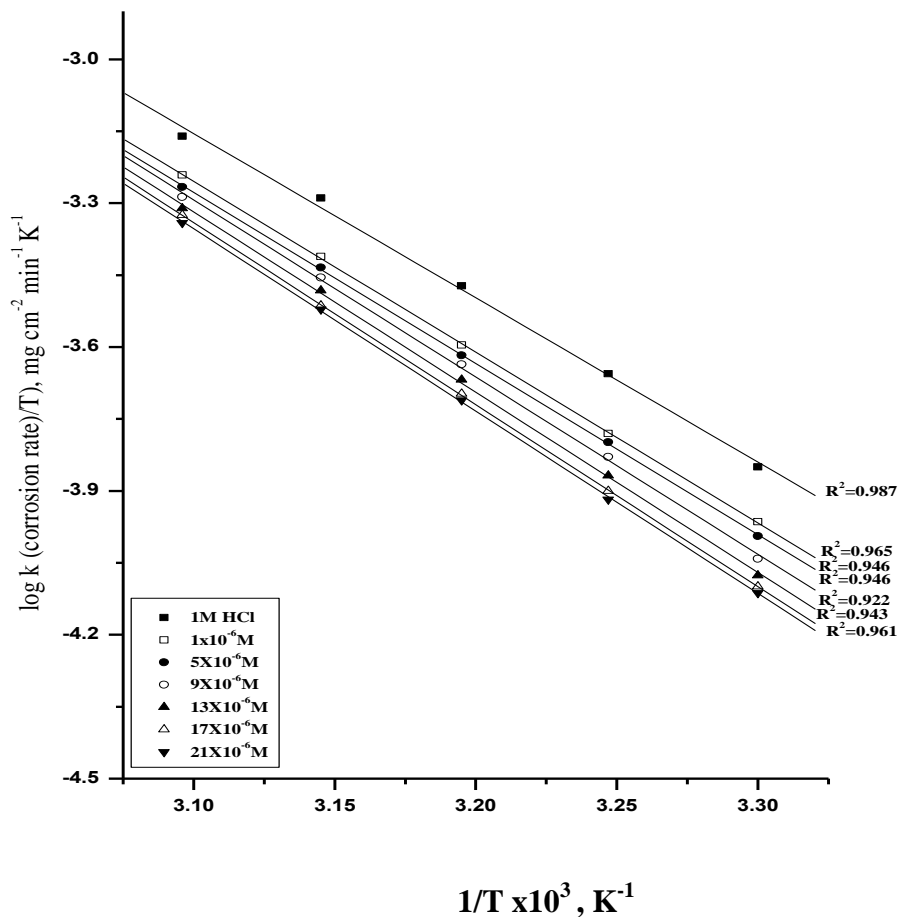


Figure 7. log (corrosion rate/T) - (1/T) curves for mild steel dissolution in 1M HCl in absence and presence of different concentrations of compound (A)

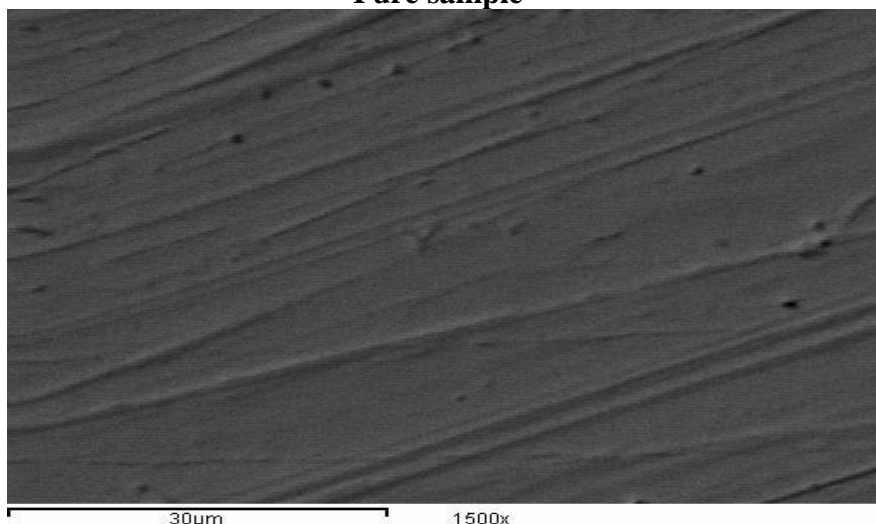
Table 6. Kinetic parameters for the dissolution of mild steel in presence and absence of different concentrations of inhibitors in 1M HCl

| Inhibitor | Conc., M. | Activation parameters | | |
|--------------------|---------------------|-----------------------|----------------------|-----------------------------------|
| | | E_a^* | ΔH^* | $-\Delta S^*$ |
| | | kJ mol^{-1} | kJ mol^{-1} | $\text{J mol}^{-1} \text{K}^{-1}$ |
| Free Acid (1M HCl) | 0.0 | 62.00 | 60.05 | 51.87 |
| (A) | 1×10^{-6} | 69.30 | 69.01 | 42.10 |
| | 5×10^{-6} | 71.12 | 71.40 | 36.01 |
| | 9×10^{-6} | 73.22 | 72.77 | 31.77 |
| | 13×10^{-6} | 76.19 | 75.46 | 23.78 |
| | 17×10^{-6} | 78.19 | 77.62 | 17.90 |
| | 21×10^{-6} | 80.02 | 78.61 | 16.02 |
| (B) | 1×10^{-6} | 65.66 | 67.00 | 47.01 |
| | 5×10^{-6} | 67.90 | 67.31 | 47.76 |
| | 9×10^{-6} | 70.33 | 69.62 | 40.43 |
| | 13×10^{-6} | 71.43 | 70.52 | 36.76 |
| | 17×10^{-6} | 72.03 | 71.53 | 35.21 |
| | 21×10^{-6} | 72.40 | 71.98 | 35.89 |

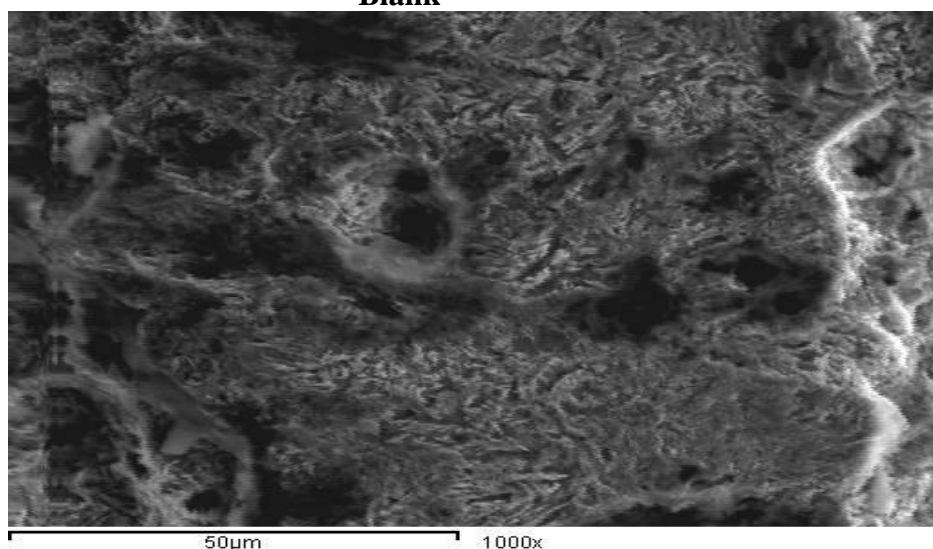
3.1.5. Scanning Electron Microscopy (SEM) Studies

Figure (8) represents the micrography obtained for mild steel samples in presence and in absence of 21×10^{-6} M phenolic derivatives after exposure for 3 days immersion. It is clear that mild steel surfaces suffer from severe corrosion attack in the blank sample. It is important to stress out that when the compound is present in the solution, the morphology of mild steel surfaces is quite different from the previous one, and the specimen surfaces were smoother. We noted the formation of a film which is distributed in a random way on the whole surface of the mild steel. This may be interpreted as due to the adsorption of the phenolic derivatives on the mild steel surface incorporating into the passive film in order to block the active site present on the mild steel surface. Or due to the involvement of inhibitor molecules in the interaction with the reaction sites of mild steel surface, resulting in a decrease in the contact between mild steel and the aggressive medium and sequentially exhibited excellent inhibition effect [38, 39].

Pure sample



Blank



Compound(A)

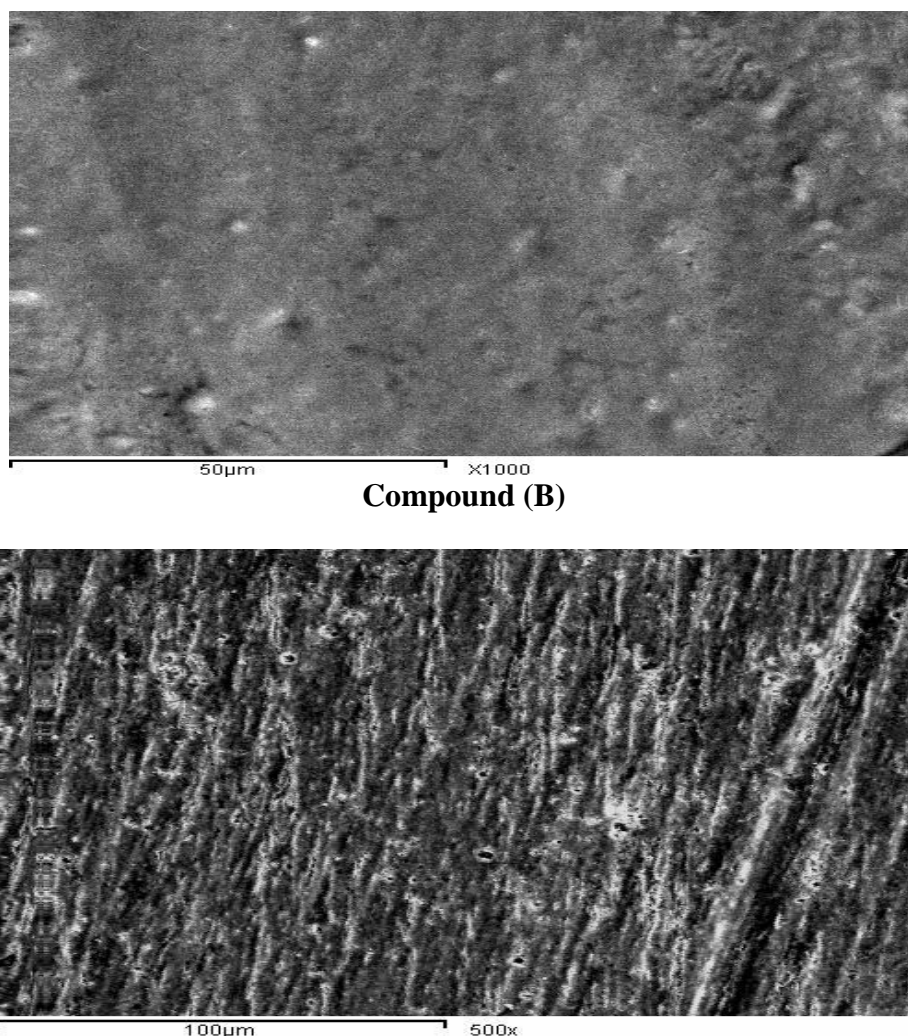
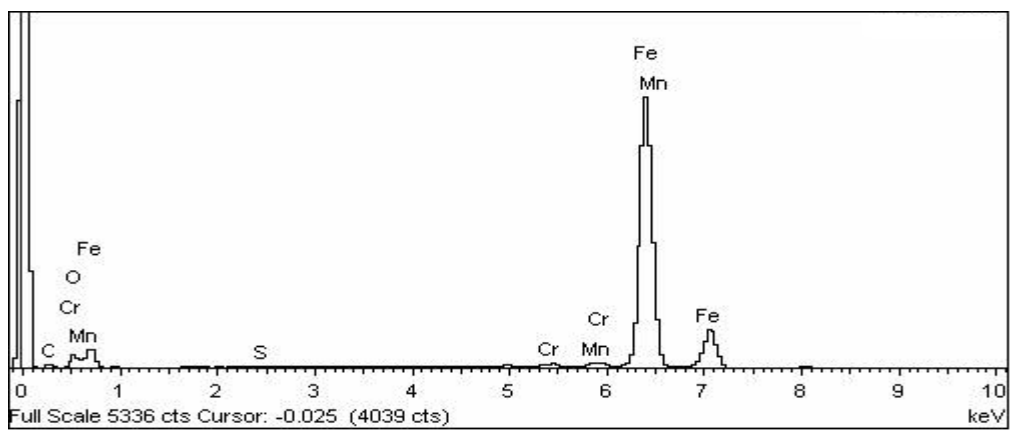


Figure 8. SEM micrographs for mild steel in absence and presence of 21×10^{-6} M of phenolic compounds.

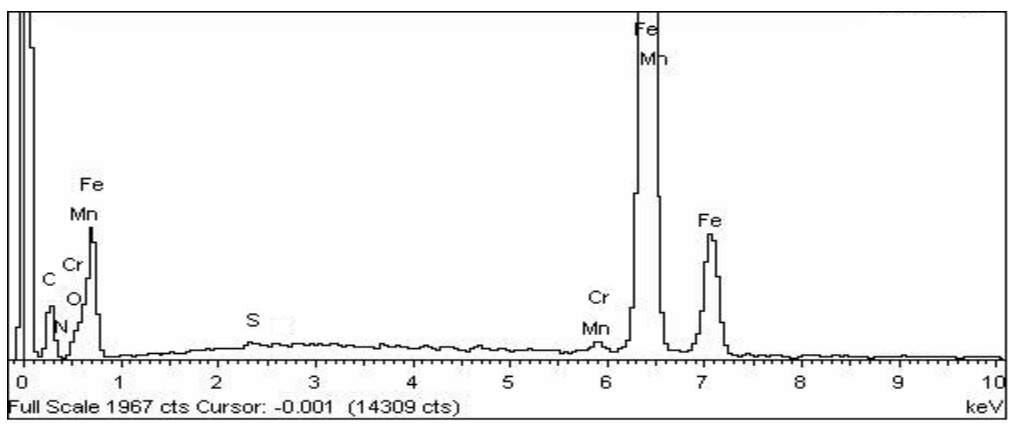
3.16. Energy Dispersion Spectroscopy (EDS) Studies

The EDS spectra were used to determine the elements present on the surface of mild steel and after 3 days of exposure in the uninhibited and inhibited 1 M HCl. Figure (9) shows the EDS analysis result on the composition of mild steel only without the acid and inhibitor treatment. The EDS analysis indicates that only Fe and oxygen were detected, which shows that the passive film contained only Fe_2O_3 . Figure (9) portrays the EDS analysis of mild steel in 1M HCl only and in the presence of 21×10^{-6} M of phenolic derivatives. The spectra show additional lines, demonstrating the existence of C (owing to the carbon atoms of phenolic derivatives). These data shows that the carbon and O atoms covered the specimen surface. This layer is entirely owing to the inhibitor, because the carbon and O signals are absent on the specimen surface exposed to uninhibited HCl. It is seen that, in addition to Mn, C, and O were present in the spectra. A comparable elemental distribution is shown in Table (7).

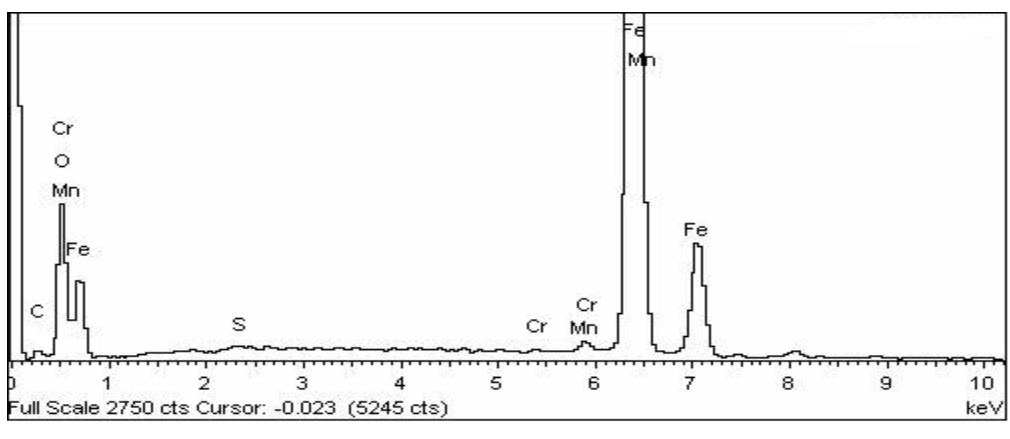
Pure sample



Blank



Compound (A)



Compound (B)

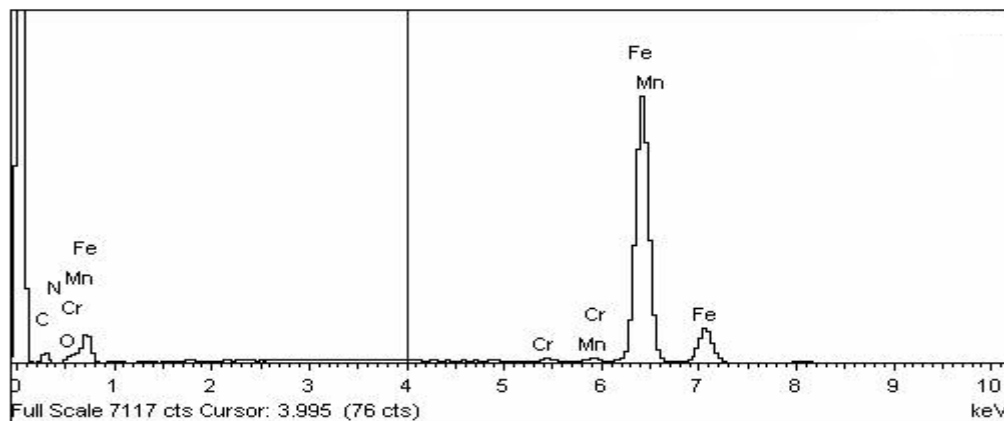


Figure 9. EDS analysis on mild steel in presence and absence of phenolic compounds for 3 days immersion

Table 7. Surface composition (wt %) of mild steel alloy after 3h of immersion in HCl without and with the optimum concentrations of the studied inhibitors

| (Mass %) | Fe | Mn | C | O | N | S | Cr |
|---------------------|-------|------|-------|-------|------|------|------|
| Pure | 97.63 | 0.64 | 1.35 | -- | -- | 0.27 | 0.11 |
| blank | 58.54 | 0.54 | 1.11 | 11.43 | 7.86 | 0.19 | 0.33 |
| Compound (A) | 67.13 | 0.60 | 21.26 | 29.21 | 1.18 | 0.21 | 0.41 |
| Compound (B) | 60.43 | 0.52 | 19.32 | 12.13 | 7.11 | 0.18 | 0.31 |

3.1.7. Quantum chemical parameters of investigated compounds

The E_{HOMO} indicates the ability of the molecule to donate electrons to an appropriated acceptor with empty molecular orbitals but E_{LUMO} indicates its ability to accept electrons. The lower the value of E_{LUMO} , the more ability of the molecule is to accept electrons [40]. While, the higher is the value of E_{HOMO} of the inhibitor, the easier is its offering electrons to the unoccupied d-orbital of metal surface and the greater is its inhibition efficiency. The calculations listed in Table (8) showed that the highest energy E_{HOMO} is assigned for the compound (A), which is expected to have the highest corrosion inhibition among the investigated compounds. The HOMO–LUMO energy gap, ΔE approach, which is an important stability index, is applied to develop theoretical models for explaining the structure and conformation barriers in many molecular systems. The smaller is the value of ΔE , the more is the probable inhibition efficiency that the compound has [41-42]. The dipole moment μ , electric field, was used to discuss and rationalize the structure. It was shown from Table (8) that compound (A) molecule has the smallest HOMO–LUMO gap compared with the other molecules. Accordingly, it could be expected that compound (A) molecule has more inclination to adsorb on the metal surface than the other molecules. The higher is the value of μ , the more is the probable inhibition efficiency that the

Variation in the inhibition efficiency of the inhibitors depends on the presence of electro negative O- and N-atoms as substituents in their molecular structure. The calculated Mulliken charges of selected atoms are presented in Fig. (10).

Table 8. Calculated quantum chemical properties for phenolic compounds

| property | compound (A) | compound (B) |
|------------------------------|--------------|---------------|
| $-E_{\text{HOMO}}$ (eV) | 8.36 | 8.51 |
| $-E_{\text{LUMO}}$ (eV) | 0.48 | 0.33 |
| ΔE (eV) | 7.880 | 8.180 |
| η (eV) | 3.940 | 4.090 |
| σ (eV ⁻¹) | 0.254 | 0.244 |
| $-\rho_i$ (eV) | 4.420 | 4.420 |
| χ (eV) | 4.420 | 4.420 |
| Dipole moment (Debye) | 4.52 | 4.29 |
| Area (Å ²) | 269.33 | 315.40 |

4. MECHANISM OF CORROSION INHIBITION

The adsorption of phenolic derivatives can be attributed to the presence of polar unit having atoms of nitrogen and oxygen and aromatic/heterocyclic rings. Therefore, the possible reaction centers are unshared electron pair of hetero-atoms and π -electrons of aromatic ring [43]. The adsorption and inhibition effect of phenolic derivatives in 1 M HCl solution can be explained as follows: In aqueous acidic solutions, phenolic derivatives exist either as neutral molecules or as protonated molecules and may adsorb on the metal/acid solution interface by one and/or more of the following ways: (i) electrostatic interaction of protonated molecules with already adsorbed chloride ions, (ii) donor-acceptor interactions between the π -electrons of aromatic ring and vacant d orbital of surface iron atoms, (iii) interaction between unshared electron pairs of hetero-atoms and vacant d-orbital of iron surface atoms. In general, two modes of adsorption are considered on the metal surface in acid media. In the first mode, the neutral molecules may be adsorbed on the surface of mild steel through the chemisorption mechanism, involving the displacement of water molecules from the mild steel surface and the sharing electrons between the hetero- atoms and iron. The inhibitor molecules can also adsorb on the mild steel surface on the basis of donor-acceptor interactions between π -electrons of the aromatic ring and vacant d-orbitals of surface iron atoms. In the second mode, since it is well known that the steel surface bears positive charge in acid solution [44], so it is difficult for the protonated molecules to approach the positively charged carbon steel surface due to the electrostatic repulsion. Since chloride ions have a smaller degree of hydration, thus they could bring excess negative charges

in the vicinity of the interface and favor more adsorption of the positively charged inhibitor molecules, the protonated phenolic derivatives adsorb through electrostatic interactions between the positively charged molecules and the negatively charged metal surface. Thus there is a synergism between adsorbed Cl^- ions and protonated phenolic derivatives. Thus we can conclude that inhibition of mild steel corrosion in 1 M HCl is mainly due to electrostatic interaction. The decrease in inhibition efficiency with rise in temperature supports electrostatic interaction.

Compound (A) has the highest percentage inhibition efficiency. This due to the presence of p-NR₂ which is an electron repelling group with negative Hammett constant ($\sigma = -0.38$). This group will increase the electron charge density on the molecule. Compound (B) comes after compound (A), this is due to the presence of p-NO₂ group which is an electron withdrawing groups with positive Hammett constants ($\sigma_{\text{NO}_2} = +0.78$) and their order of inhibition depends on the magnitude of their withdrawing character.

5. CONCLUSIONS

- The phenolic derivatives inhibit the corrosion of mild steel in 1 M HCl.
- The inhibition is due to adsorption of the inhibitor molecules on the mild steel surface by Blocking its active sites.
- Adsorption of phenolic derivatives fits Frumkin isotherm.
- Results obtained from weight loss, DC polarization, and AC impedance techniques are reasonably in good agreement and show increased inhibitor efficiency with increasing inhibitor concentration.
- Polarization data showed that the used inhibitors act as mixed-type inhibitor in 1 M HCl.

References

1. M.A. Deyab, *Corros. Sci.* 49 (2007) 2315.
2. S.A. Abd El-Maksoud A.S. Fouda, *Mater.Chem.phys.*93 (2005) 84.
3. K.F.Khaled, *Mater. Chem.phys.* 122(2008) 290.
4. E.Machnikova,K.H. Whitmire and N Hackeman, *Electrochim. Acta* 53 (2008) 6024.
5. H Ashassi-sorkhabi, M.R. Magidi and K. Seyyedi, *Appt. Surf. Sci.*225 (2004) 176.
6. M.A. Migahed and I.F. Nasser, *Electrochim. Acta* 53 (2008) 2877.
7. G.Avci, *Colloids Surf. A* 317 (2008)730.
8. K.C.Pillali and R.Narayan, *Corros.Sci.*, 23 (1985) 151
9. A.B.Tadros and B.A.Abdel-Naby, *J.Electroanal.Chem.*, 224(1988) 433.
10. JO'M.Bockris and B.Yang, *J.Electrochem.Soc.*, 138(1991) 2237.
11. V.Jovancicevic, B.Yang and JO'M.Bockris, *J.Electrochem.Soc.*, 135(1989) 94
12. J.Uhera and K.Aramaki, *J.Electrochem.Soc.*, 138(1991)3245.
13. A.A.Akust, W.J.Lorenz and F.Mansfeld, *Corros.Sci.*, 22(1982) 611.
14. M. Abdallah, E. A. Helal and A. S. Fouda *Corros. Sci.*, 48 (2006) 1639.
15. A. S. Fouda, A. A. Al-Sarawy and E. E. El-Katori. *Chem. Paper*, 60(1) (2006) 5.
16. A. S. Fouda, A. A. Al-Sarawy and E. E. El-Katori. *Desalination J.*, 201 (2006) 1.
17. O.Benali, L. Larabi, M Traisnel, L. Gengembra, Y. Harwk, *Appi. Surf. Sci* 253(2007)6130.
18. M.A. Khalifa,M.El-Batouti, F.Mhgoub,A.Bakr Aknish,*Mater.Corrps.*54 (2003) 251.

19. Y. Abboud, A. Abourriche, T. Saffag, M. Berrada, M. Charrouf, A. Bennamara, N. Al Himidi and H. Hannache, *Mater. Chem. Phys.* 105 (2007) 1.
20. K.F. Khaled, *Electrochim. Acta* 48 (2003) 2493.
21. A. Popova, M. Chistov, S. Raicheva and E. Sokolova, *Corros. Sci.* 46(2004)1333.
22. E.A. Noot and A.H. Al-Moubaraki, *Mater. Chem. Phys.* 110 (2008) 145.
23. C.M. Yan, H.Y. Cheng, T.C. Lin. *J. Ethnopharmacol.* 110 (2007) 555.
24. M. Ajmal, A.S. Mideen, and M.A. Quraishi, *Corros. Sci.*, 36 (1994) 79.
25. F. Bentiss, M. Lebrini and M. Lagrenée. *Corros. Sci.*, 47 (2005) 2915.
26. M. El Achouri, S. Kertit, H.M. Goultaya, B. Nciri, Y. Bensouda, L. Perez, M.R. Infante and K. Elkacemi, *Prog. Org. Coat.*, 43 (2001) 267.
27. K.F. Khaled, *Electrochim. Acta*, 48 (2003) 2493.
28. F.B. Growcock and J.H. Jasinski, *J. Electrochem. Soc.*, 136 (1989) 2310
29. U. Rammet and G. Reinhart, *Corros. Sci.*, 27 (1987) 373.
30. A.H. Mehaute and G. Grepy, *Solid State Ionics* 9–10 (1983) 17.
31. E. Machnikova, M. Pazderova, M. Bazzaoui and N. Hackerman, *Surf. Coat. Technol.*, 202 (2008) 1543.
32. C.H. Hsu and F. Mansfeld, *Corrosion*, 57 (2001) 747.
33. M. Lebrini, M. Lagrenée, M. Traisnel, L. Gengembre, H. Vezin and F. Bentiss, *Appl. Surf. Sci.*, 253 (2007) 9267
34. R.W. Bosch, J. Hubrecht, W.F. Bogaerts and B.C. Syrett, *Corrosion*, 57 (2001) 60.
35. Gamry Echem Analyst Manual, 2003.
36. R.G. Kelly, J.R. Scully, D.W. Shoesmith and R.G. Buchheit, *Electrochemical Techniques in Corrosion Science and Engineering*, Marcel Dekker, Inc., New York, (2002) 148.
37. G.B. Ateya, B. El-Anadouli, and F. El-Nizamy, *Corros. Sci.*, 24 (1984) 509.
38. R.A., Prabhu, T.V., Venkatesha, A.V., Shanbhag, G.M., Kulkarni, R.G., Kalkhambkar, *Corros. Sci.*, 50 (2008) 3356.
39. G., Moretti, G., Quartanone, A., Tassan, A., Zingales, *Wkst. Korros.*, 45 (1994) 641
40. G. Gao, C. Liang, *Electrochim. Acta.*, 52 (2007) 4554.
41. G. Gece, S. Bilgic. *Corros. Sci.*, 51 (2009) 1876.
42. S. Martinez. *Mater. Chem. Phys.*, 77 (2002) 97.
43. Ishtiaque Ahmad, Rajendra Prasad and M.A. Quraishi, *Corros. Sci.*, 52 (2010) 3033.
44. Ashish Kumar Singh and M.A. Quraishi, *Corros. Sci.*, 52 (2010) 1529.